Advanced Antenna Design For NASA's EcoSAR Instrument

Cornelis F. du Toit
AS and D, Inc., work performed for NASA/GSFC
Greenbelt, MD 20770

Manohar Deshpande, Rafael F. Rincon
NASA/Goddard Space Flight Center
Greenbelt, MD 20770

***Abstract* — Advanced antenna arrays were designed for NASA's EcoSAR airborne radar instrument. EcoSAR is a beamforming synthetic aperture radar instrument designed to make polarimetric and "single pass" interferometric measurements of Earth surface parameters. EcoSAR's operational requirements of a 435MHz center frequency with up to 200MHz bandwidth, dual polarization, high cross-polarization isolation (> 30 dB), ± 45° beam scan range and antenna form-factor constraints imposed stringent requirements on the antenna design. The EcoSAR project successfully developed, characterized, and tested two array antennas in an anechoic chamber. EcoSAR's first airborne campaign conducted in the spring of 2014 generated rich data sets of scientific and engineering value, demonstrating the successful operation of the antennas.**

Keywords—SAR; phased array, antennas; InSAR; Pol-InSAR; digital beamforming; polarimetry; P-band; wideband.

I. Introduction

EcoSAR is a beamforming synthetic aperture radar (SAR) instrument developed at the NASA/ Goddard Space Flight Center (GSFC) as a part of NASA's Earth Science Technology Office (ESTO) Instrument Incubator Program (IIP). The instrument was designed to make polarimetric and "single pass" interferometric measurements of ecosystem structure and biomass [1][2] from a platform on board a P3 aircraft (see Fig. 1). The instrument employs an advanced wideband multi-channel radar architecture that allows considerable measurement flexibility and enables imaging techniques beyond the capabilities of conventional SAR systems [3].

EcoSAR operates in the P-band with a center frequency of 435 MHz (69 cm wavelength) at four polarizations (HH, VV, HV, and VH) using two array antennas. The EcoSAR signals propagate through vegetation structure, providing information about the vegetation's three-dimensional distribution and density. Thus, EcoSAR has the unique capability of mapping above-ground structure and biomass, disturbance from deforestation and degradation, forest recovery, and wetland inundation. EcoSAR measurements are also suitable for several other critically important science applications, including permafrost change, soil moisture, ice dynamics, glacier depth, and crop and land cover monitoring. The EcoSAR measurements directly support science studies recommended by the National Science Foundation's Decadal Survey [4] and highlighted in NASA's Plan for a Climate-Centric Architecture [5].

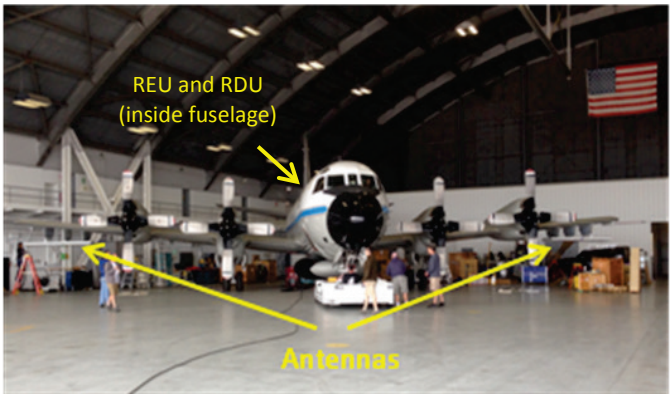

Fig. 1 The EcoSAR instrument, designed to fly on a P3 aircraft, is a polarimetric and single pass interferometric SAR instrument that employs an advanced multichannel digital and analogue architecture and two wing-mounted array antennas with a baseline of 25 m. (REU: Radar Electronics Unit, RDU: Radar Digital Unit).

EcoSAR employs multiple-input multiple output (MIMO) radar architecture that allows the implementation of advanced imaging techniques. Its reconfigurable architecture allows the real-time selection of radar parameters, including center frequency, bandwidth (range resolution), incidence angle, transmit beam characteristics (beamwidth and side-lobes level), among others.

The EcoSAR architecture comprises three main subsystems: the Radar Digital Unit (RDU), the Radar Electronics Unit (REU), and the antennas, as illustrated in Fig. 2.

- The RDU is a custom FPGA-based processor system capable of multi-channel arbitrary waveform generation, data acquisition, and on-board processing.
- The REU is made up 32 transmit/receive (T/R) modules that condition radar signals and provide several radar system calibrations schemes. The receivers also provide high dynamic range to avoid saturation due to strong specular reflection from nadir.
- The antenna subsystem consists of two dual-polarization array antennas, each mounted under one of the aircraft wings to providing an interferometric baseline of 25m. The antennas are capable of beam steering / beam forming in the cross-track plane. With the main beams steered away from nadir, low sidelobe levels together with null-

steering toward nadir minimize the expected strong specular reflection of the radar signal.

A more detailed description of each subsystem is given by Rincon et al [1]. Performance parameters and characteristics achieved with EcoSAR are listed on Table I.

EcoSAR's first flight campaign took place in March 2014 over areas of the Bahamas and Costa Rica. The instrument flew 19 hours (including transit) on-board the National Oceanic and Atmospheric Agency (NOAA) WP-3D Orion "Hurricane Hunter" aircraft, shown in Fig. 1. The aircraft was specifically commissioned for EcoSAR's flight certification, tests, and science campaign. During the campaign, EcoSAR operated in several experimental modes and acquired data for calibration, performance assessment, and science analysis.

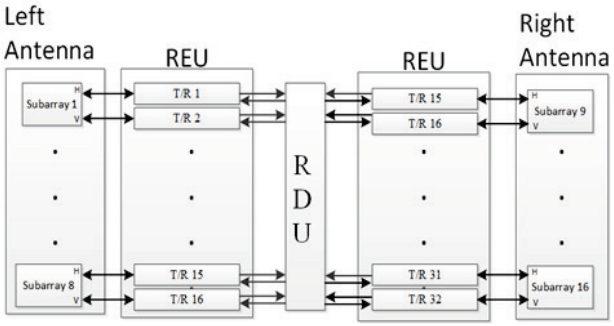

Fig. 2: EcoSAR's multi-channel beamforming architecture.

TABLE I. ECOSAR'S MAIN CHARACTERISTICS

Center Frequency	435 MHz
Maximum Bandwidth	200 MHz
Polarization	Full
Polarization Isolation	> 30 dB
Noise Equivalent σ_o	- 41 dB *
Total Number Channels	32
Interferometric baseline	25 m
Pulse Length	1 μsec – 50 μsec
Array Peak Power/polarization	40 Watts
PRF	100 Hz – 10 KHz
Swath	4 km *
Finest Range Resolution	0.75 m
Single Look Azimuth Resolution	0.5 m
Vertical Accuracy	< 5 m

* nominal operation

The demand for state of the art wide band antennas in the UHF and P-band has lately been driven by the earth sciences and other desciplines due to the deep penetration capabilities at these frequencies. Guinvarc'h and Ribière-Tharaud [6] pursued a single wideband element antenna for airborne SAR; Thomas [7] describes a wide band UHF antenna array for the GeoSAR program, while Ren et al. [8] developed a low frequency array for wall penetration radar, to name but a few examples.

Initial work on the EcoSAR antenna array element investigated a single patch resonator, capacitively coupled to large vertical feed posts [9][10]. This element showed promising wide band capability, but in the restrictive array environment required a more involved matching network. To eliminate the need for two 180° power dividers per element, the final element design focused on an aperture coupled stacked patch approach [11]. To avoid the need of a bulky supporting substrate at P-band, a design was pursued featuring supporting dielectric posts and non-planar patches for improved mechanical strength, similar to earlier concepts described by Du Toit et al.[12].

In the next few sections, the antenna design is discussed, followed by a report on the RF performance measurement results.

II. ANTENNA DESIGN

A. Antenna Requirements

The system requirements are for two dual polarized P-band antenna arrays, separated by a baseline of about 25m for interferometric purposes. The two antennas are to be mounted on the port side and starboard side wings of an aircraft, facing towards nadir. With a center operating frequency of 435MHz, a large bandwidth >100MHz (200MHz goal) is required for high cross track (right angles to the flight path) resolution, utilizing cross track beam steering of up to 35° from nadir. The antenna beamwidth in the cross-track plane is required to be less than 18° at 435MHz, while the beam is scanned to boresight. In the along-track plane, the beam width is linked to the along track antenna length, which was constrained by size limitations of the aerodynamic enclosure [13] to a maximum of 80cm. The compromise is that a shorter along-track antenna length increases the pulse repetition frequency and integration time of the SAR system. As a result, the along-track plane beamwidth associated with an 80cm antenna dimension is expected to be about 50° at 435MHz. Finally, high isolation >30dB between the antenna arrays' dual polarization ports, and low cross-polarization pattern levels <–30dB in the principle planes are also required.

B. Antenna Geometry

For synthetic aperture purposes, it is sufficient for each array to use two elements with 40cm separation in the flight path direction. To keep within the 18° cross-track beamwidth requirement while preventing grating lobes, 8 active elements spaced 29cm apart along the cross-track direction is deemed sufficient. The fully assembled array is shown in Fig. 3, together with a schematic of a single 2-element pair.

Each element is based on a stacked, non-planar patch design [12]. The elements are fed with an aperture-coupled arrangement [14] for vertical (V) polarization (E-plane aligned cross-track, or along the long dimension of the array), and a probe-fed arrangement for the horizontal (H) polarization excitation (E-plane aligned along-track, or along the short dimension of the array). The definitions of the V- and H-polarizations derives from the fact that when the antenna beam is scanned cross-track away from nadir, the V-polarization electrical field vector will have a vertical component, while the H-polarization E-field vector will be horizontal.

The vertical polarization excitation uses a simple microstrip power divider and strip-aperture coupler circuit, while the horizontal polarization excitation is done via a strip-to-slot-to-strip coupler/divider circuit technique. Pairs of elements are constructed as separate sub-array units, each with its own integrated feed network, as shown in Fig. 4. As such, these sub-array units act as single "elements" in a linear phased array system.

To improve the end elements' active S-parameters, the EcoSAR arrays are flanked by one inactive sub-array unit at each end, for a total 2×10 elements in each array.

The final antenna design was described in a NASA New Technology Report [15].

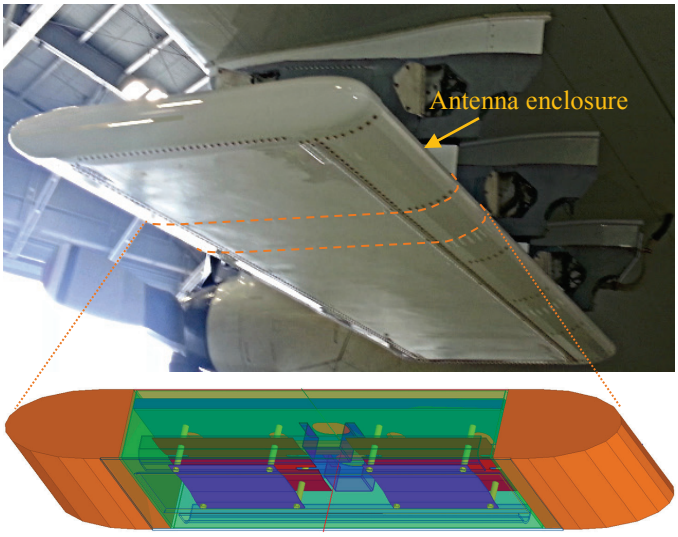

Fig. 3: One of the EcoSAR arrays mounted below the wing of an airplane, with a schematic of a sub-array pair of elements. The complete assembly is about 3.3m × 1.34 × 0.16m.

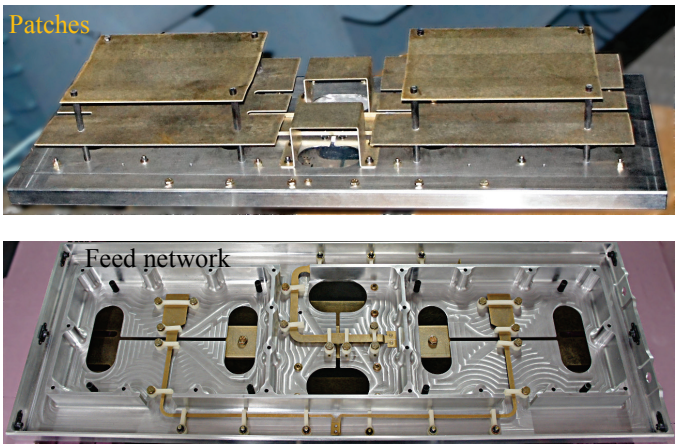

Fig. 4: One sub-array of two elements with their own integrated feed network.

C. *Design Challenges*

The large 46% desirable bandwidth requirement and the need for a moderately wide ±35° beam steering angle, are extremely challenging requirements from an antenna design point of view. The beam steering requirement limits the antenna element spacing to about half a wavelength at the highest frequency, to prevent grating lobes. As a result, the element spacing is significantly less than half a wavelength at the lower end of the band, with associated higher mutual coupling effects. In contrast, a wide bandwidth typically requires a larger antenna volume.

Instead of working against mutual coupling by trying to minimize it, wide band phased array performance can in fact be improved by utilizing strong coupling between elements under the right conditions, as described by Chen et al. [16]. The strong field coupling allows adjacent elements to share surrounding space through mutually coupled fields, thereby improving the bandwidth. This is reminiscent of the strong coupling required between the elements of a frequency selective surface [17], which is necessary for wide band reflectivity over a wide range of incidence angles. The EcoSAR antenna design takes advantage of the strong mutual coupling between elements in a similar way, thereby achieving wide band performance, especially in the vertical polarization excitation. The horizontal polarization bandwidth was somewhat compromised by the bandwidth of the strip-to-slot-to-strip coupler/divider circuit. The shorter antenna dimension in the E-plane of the H-polarization excitation vs the case for the V-polarization excitation also lead to comparatively less favorable mutual coupling conditions, which contributed to the reduced H-polarization bandwidth.

The aerodynamical antenna enclosure also imposed restrictions on the along-track beam shape and back lobes. Nevertheless, the front to back ratio (F/B) for the horizontal polarization was maximized to be more than 25dB, while the vertical polarization F/B achieved more than 15dB. The back lobes are of concern since they can scatter off the aircraft wings and mounting structures, causing interference with the main beam. Even with a F/B ratio of 15dB, the back lobe scattering is expected to be more than 20dB below the main beam peak, which is similar to the sidelobe level achievable through beam forming.

Installation of the sub-array units into the aerodynamical enclosure posed additional RF grounding challenges. Improper grounding causes unexpected resonances, compromising return loss and decreasing isolation between the two orthogonal polarization excitations. As slide-in mechanical design had to be refined with numerous spring-loaded contact points to improve grounding along the periphery of each sub-array unit.

III. Antenna Performance

A. *Impedance Bandwidth*

In spite of the design challenges, a 200MHz bandwidth was achieved for the vertical polarization. For horizontal polarization, a 120MHz bandwidth was achieved, as shown in Fig. 5 for the case when the antenna is scanned to nadir. At higher scan angles, the active S-parameters deteriorates, with the vertical polarization ports still achieving –9dB or better over the 200MHz band at ±35° scanning, as shown in Fig. 6.

Under the same conditions, the horizontal polarization ports achieve −7dB or better over the 120MHz band. These high active port reflection levels are only associated with the less excited elements near the ends of the array, with the central elements typically exhibiting port reflection levels lower than −10dB. As a result, the overall reduction in gain due to port mismatches at the extreme scan angles are still less than 0.5dB.

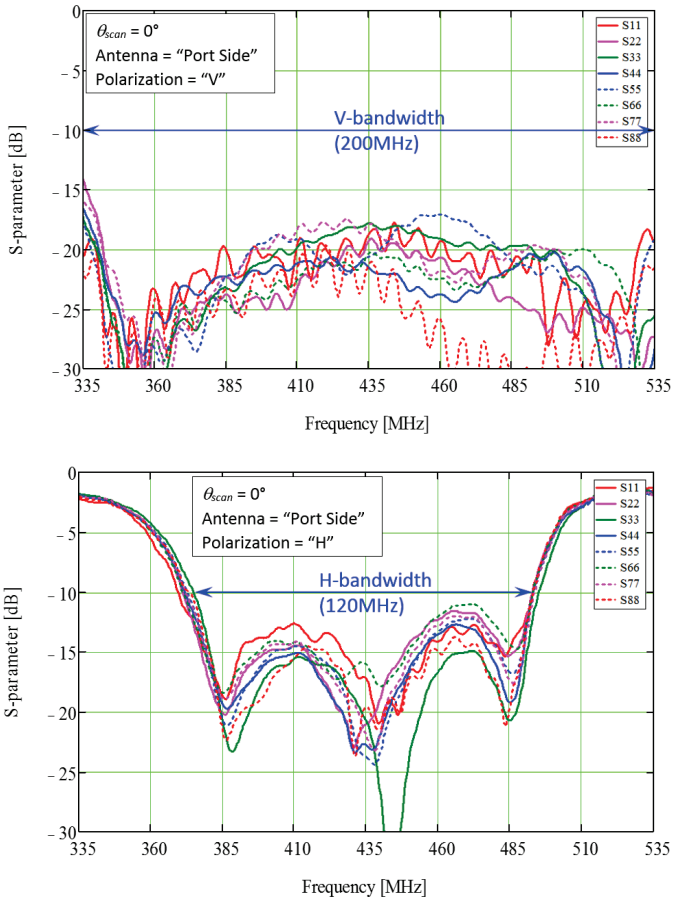

Fig. 5: Measured *active* S-parameters for the port-side array, during 0° scan angle (from nadir) conditions.

The typical behavior of the active S-parameters over scan angle is illustrated in Fig. 7 for the center frequency. The active S-parameter sensitivity to the scan angle is driven by mutual coupling between the sub-array units, which are shown in Fig. 8. Adjacent element coupling is generally below −15dB for both polarizations, while the narrower "H"-polarization port bandwidth is clearly noticeable in the plots. Isolation between the "H" and "V" ports within each subarray unit is better than 29dB, and around 40dB over large parts of the operating bandwidth, as shown in Fig. 9. The "H" and "V" port coupling across different sub-array units (not shown here) is significantly lower.

B. Antenna pattern measurements

Active sub-array unit patterns of the port side and starboard side EcoSAR array antennas were measured in a large anechoic chamber using a P-band standard gain horn. Measurement results for the port side antenna only will be shown here, as the starboard results are the same within experimental error. Active sub-array patterns are shown in Fig. 10 for the center operating frequency in the scan plane (cross-track). The patterns show the characteristic expected cosine taper, with peak gains varying between 5dBi and 7dBi.

Since the EcoSAR antennas are active arrays, the measured active sub array unit patterns have to be combined analytically to show the full synthesized array patterns. For the example patterns shown here, a typical cosine square on a 0.2 pedestal power excitation profile is used:

The amplitude and phase of the excitation weights are also corrected through a simple calibration scheme, wherein the *average* phase and amplitude differences in the active element patterns over the scan angle and frequency ranges are removed. Finally, the correct time delay equivalent phase is applied to the excitation weights to scan the main beam off-boresight in the cross-track plane.

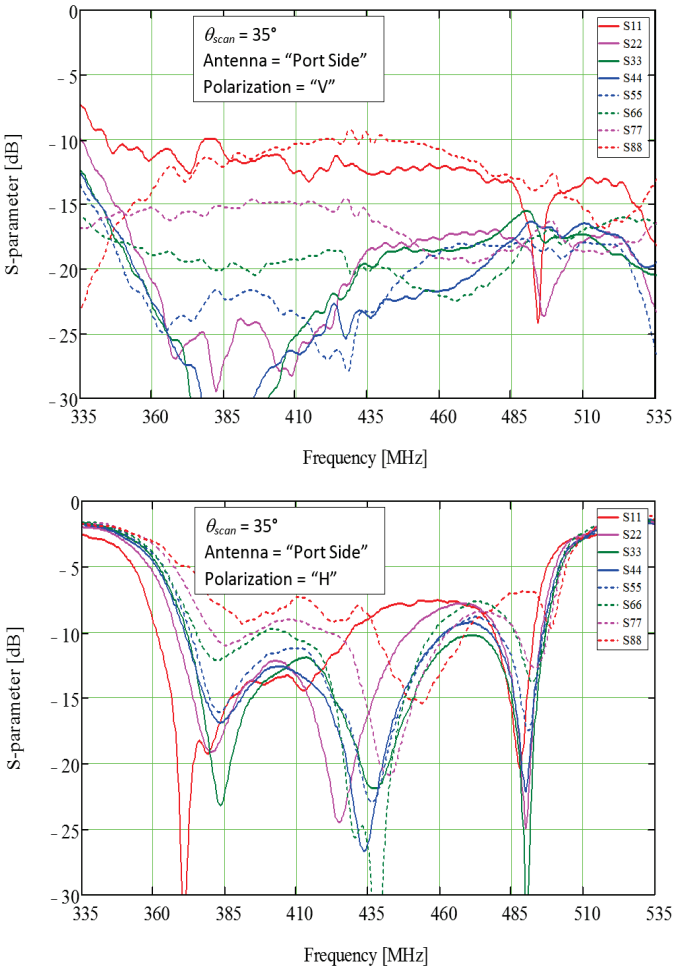

Fig. 6: Measured *active* S-parameters for the port-side array, during 35° scan angle (from nadir) conditions.

Along track, the array patterns exhibit broad ~50° half power beam widths as shown in Fig. 11 for the scan angle set to 0°. The beam width stays roughly the same for other scan angles. In the cross track or scan plane, the synthesized array

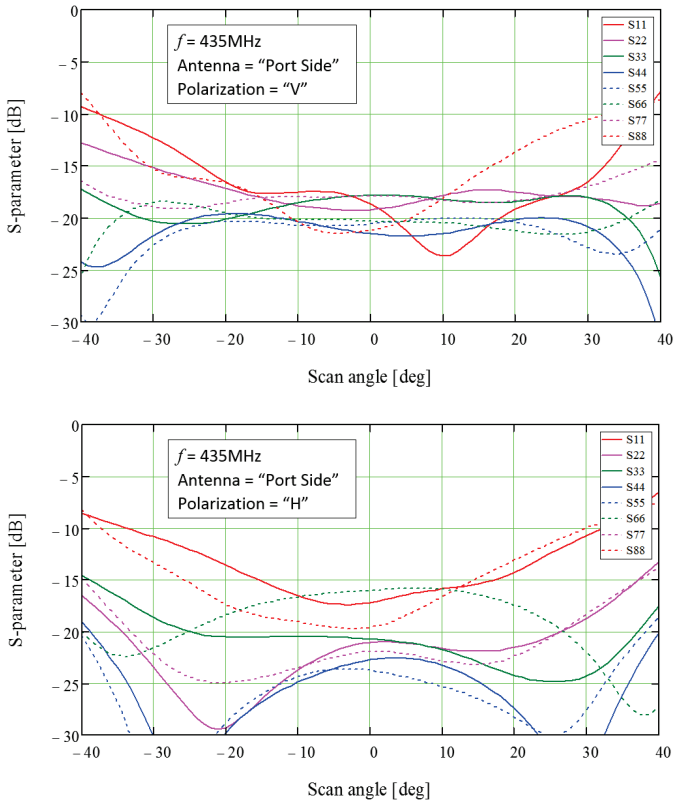

Fig. 7: Measured *active* S-parameters for the port-side array, as functions of the scan angle (from nadir), for 435MHz.

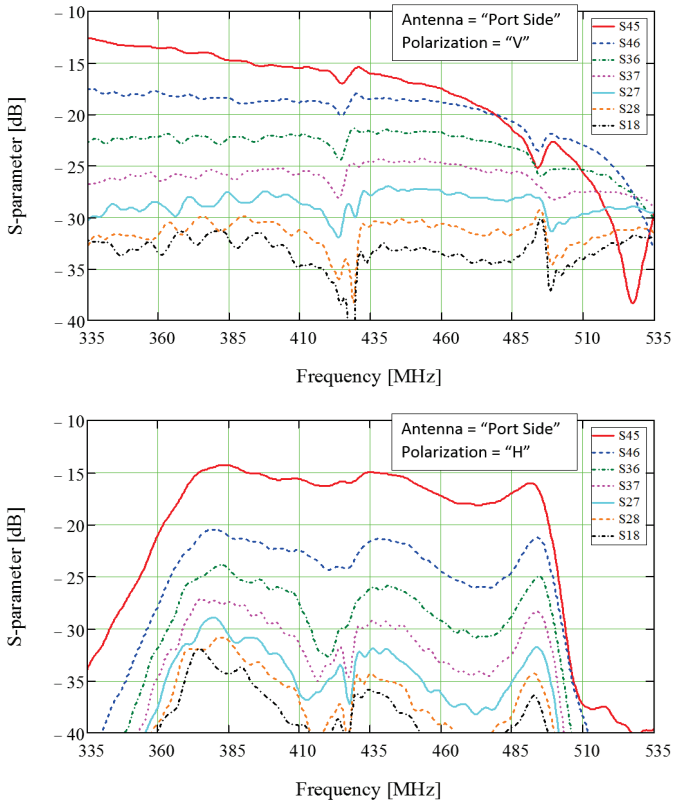

Fig. 8: Mutual coupling measurements of the port-side array, between selected pairs of sub-array units.

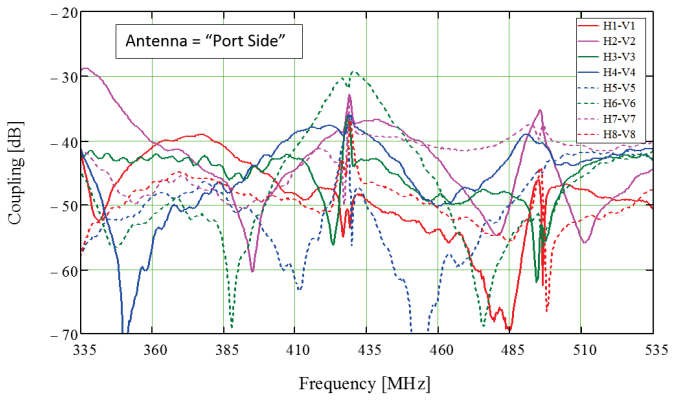

Fig. 9: Cross-coupling measurements within sub-array units of the port-side array antenna.

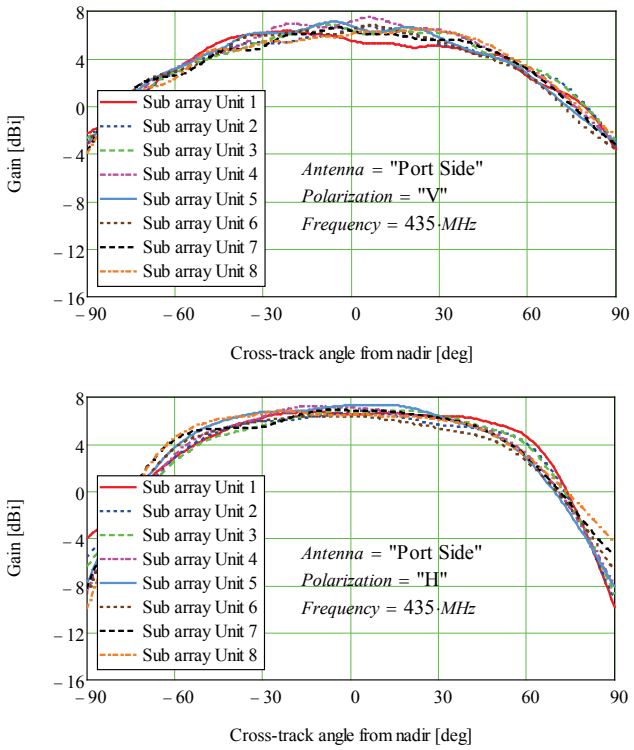

Fig. 10: Active cross-track sub-array unit pattern measurements at 435MHz

patterns exhibit the expected narrow main beam and low sidelobes, as shown in Fig. 12 for 435MHz.

C. *Flight campaign measurements*

The EcoSAR system was finally used to perform measurements over some forested areas on Andros Island in the Bahamas during a flight campaign in March 2014. Fig. 13 shows some of the images acquired. The high resolution achieved shows that the synthetic aperture synthesis, cross-track array beam scanning, data acquisition and processing was executed successfully.

CONCLUSIONS

The EcoSAR system and antenna configuration for the remote sensing of biomass has been described. Aspects and

design challenges of the wide band antenna array design for P-band have been discussed, followed by presentation of the antenna S-parameter and pattern measurement results. The antenna array is shown to be capable of scanning up to 35° off boresight without significant deterioration in gain and port return loss. The system has been flown and tested in a flight campaign, successfully demonstrating antenna array beam forming, synthetic aperture radar operation, data acquisition and processing to obtain high-resolution radar images.

For the flight campaign, a simple element amplitude and phase calibration scheme was used. The active element gain patterns, as functions of frequency and scan angle, can be used as calibration curves in future radar refinement in more sophisticated ways to improve pattern synthesis. In addition, any long term changes in the active S-parameter behavior directly affects the active insertion loss/gain of each sub-array unit. Future work can therefore also investigate the possibility of S-parameter monitoring during flight campaigns to update the element gain calibration in real time.

ACKNOWLEDGMENT

The EcoSAR development and flight campaign was possible through a NASA Earth Science Technology (ESTO) Instrument Incubator Program (IIP) award. Special thanks to the National Oceanic and Atmospheric Administration (NOAA) Aircraft Operations Center for the outstanding support in the integration of the EcoSAR instrument to the NOAA P3 aircraft and in the conduct of the EcoSAR flights.

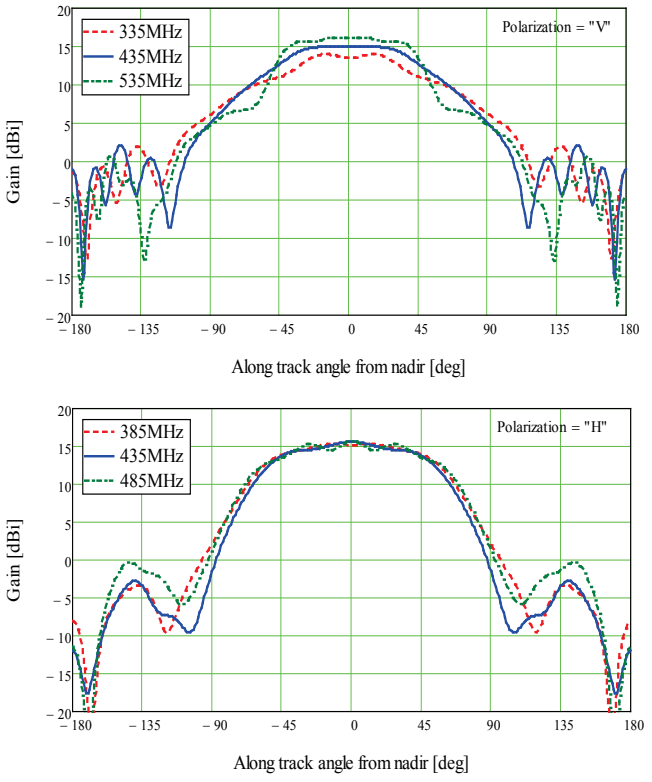

Fig. 11: EcoSAR array patterns along track, scan angle = 0°.

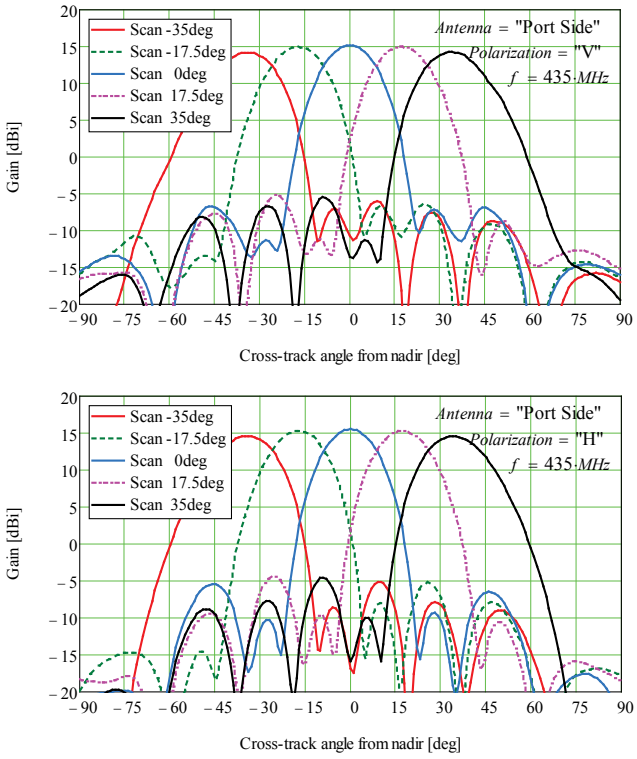

Fig. 12: EcoSAR corss-track scanned array patterns at 435MHz. The array excitation

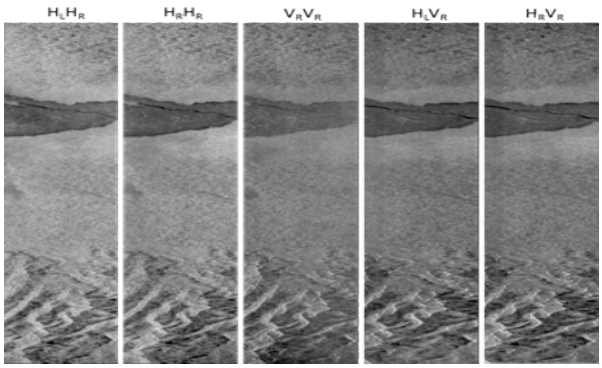

Fig. 13: EcoSAR's co-pol (HH and VV) and cross-pol (HV) images acquired on the left (L) and right (R) side of the aircraft.

REFERENCES

[1] R. Rincon, T. Fatoyinbo, K. Ranson, B. Osmanoglu, G. Sun, M. Deshpande, M. Perrine, C. Du Toit, Q. Bonds, J. Beck, and D. Lu, "The ecosystems sar (EcoSAR) an airborne P-band polarimetric InSAR for the measurement of vegetation structure, biomass and permafrost," *Proc. 2014 IEEE Radar Conference*, pp. 1443–1445, May 2014, Cincinnati OH, USA

[2] T. Fatoyinbo, R. F. Rincon, G. Sun and K. J. Ranson, "EcoSAR: A P-band digital beamforming polarimetric interferemetric SAR instrument to measure ecosystem structure and biomass," *Proc. IEEE Int. Geosci. Rem. Sens. Symp.*, July 25-29, 2011, Vancouver, Canada.

[3] R. F. Rincon, M. A. Vega; M. Buenfil, A. Geist, L. Hilliard and P. Racette, "NASA's L-band digital beamforming synthetic aperture radar," *IEEE Transactions on Geoscience and Remote Sensing*, vol.49, no.10, pp.3622-3628, Oct. 2011. doi: 10.1109/TGRS.2011.2157971.

[4] Earth science and applications from space: National imperatives for the next decade and beyond. Committee on earth science and applications from space: A community assessment and strategy for the future, National Research Council (ESDS, 2007). Responding to the challenge of climate and environmental change: NASA's plan for a climate-centric architecture for earth observations and applications from space, June 2010.

[5] Responding to the Challenge of Climate and Environmental Change: NASA's Plan for a Climate-Centric Architecture for Earth Observations and Applications from Space, June 2010, Washington, D.C

[6] R. Guinvarc'h and N. Ribière-Tharaud, "A wideband antenna for P-band airborne SAR applications," *Proc. IEEE AP-S Symp.*, San Diego, CA, Jul. 5–12, 2008R.

[7] R. F. Thomas, "Ultra-wideband UHF microstrip array for GeoSAR application," *Proc. IEEE AP-S Int. Symp.*,Atlanta, GA, Jun. 1998.

[8] Y.-J. Ren, C.-P. Lai, P.-H. Chen and R. M. Narayanan, "Compact ultrawideband UHF array antenna for through-wall radar applications," *IEEE Antennas And Wireless Propagation Letters*, Vol. 8, 2009.

[9] M. Deshpande, Q. Bonds and R. F. Rincon, "Design and validation of wideband dual polarized P-band antenna for NASA/GSFC's EcoSAR radar, " *Proc. IEEE Int. Geoscience and Remote Sensing Symp*., July 2012, Munich, Germany.

[10] A. Eslami, J. Lee Jr, H. Mishoe, J. Luttamaguzi, E. Sheybani and M. Deshpande "Development of wideband dual polarized of microstrip antennas for microwave remote sensing," *Proc. International Conference on Advances in Satellite and Space Comm.*, April 2013, Venice, Italy.

[11] D. Pozar, "A microstrip antenna aperture coupled to a microstripline," *Electronics Letters*, vol. 21. Jan. 1985, pp. 49-50.

[12] C. F. du Toit, M. M. E. Ehlen, R. J. Hutchinson and J. H. Thomson, Dual polarized patch-radiating element," US Patent No. 6236367 B1, May 2001.

[13] Hale, N. Roberts, W. Liu, M. Yang, D. Schroer and B. Kaushhik, "Flight safety review: EcoSAR integration on the NASA P-3," NASA internal document, June 2013.

[14] C. F. du Toit, "Stacked patch antenna," US. Patent No. 7109926 B2. Sep. 2006.

[15] C. F. du Toit, "Ultra-wideband, dual-polarized, beam-steering P-band array antenna," *NASA NTR* GSC-16778-1, Jan. 2014.

[16] Y. Chen, S. Yang and Z. Nie, "A novel wideband antenna array with tightly coupled octagonal ring elements," *Progress in Electromagnetics Research*, Vol. 124, p55-70, 2012.

[17] B. A. Munk, *Frequency selective surfaces*, John Wiley & Sons, Inc. New York, 2000.